Science in China Series B: Chemistry

Theoretical study of the N—H···O red-shifted and blue-shifted hydrogen bonds

YANG Yong†, ZHANG WeiJun, PEI ShiXin, SHAO Jie, HUANG Wei & GAO XiaoMing

Laboratory of Environmental Spectroscopy, Anhui Institute of Optics and Fine Mechanics, Chinese Academy of Sciences, Hefei 230031, China

Theoretical calculations are performed to study the nature of the hydrogen bonds in complexes HCHO···HNO, HCOOH···HNO, HCHO···NH_3, HCOOH···NH_3, HCHO···NH_2F and HCOOH···NH_2F. The geometric structures and vibrational frequencies of these six complexes at the MP2/6-31+G(d,p), MP2/6-311++G(d,p), B3LYP/6-31+G(d,p) and B3LYP/6-311++G(d,p) levels are calculated by standard and counterpoise-corrected methods, respectively. The results indicate that in complexes HCHO···HNO and HCOOH···HNO the N—H bond is strongly contracted and N—H···O blue-shifted hydrogen bonds are observed. While in complexes HCHO···NH_3, HCOOH···NH_3, HCHO···NH_2F and HCOOH···NH_2F, the N—H bond is elongated and N—H···O red-shifted hydrogen bonds are found. From the natural bond orbital analysis it can be seen that the X—H bond length in the X—H···Y hydrogen bond is controlled by a balance of four main factors in the opposite directions: hyperconjugation, electron density redistribution, rehybridization and structural reorganization. Among them hyperconjugation has the effect of elongating the X—H bond, and the other three factors belong to the bond shortening effects. In complexes HCHO···HNO and HCOOH···HNO, the shortening effects dominate which lead to the blue shift of the N—H stretching frequencies. In complexes HCHO···NH_3, HCOOH···NH_3, HCHO···NH_2F and HCOOH···NH_2F where elongating effects are dominant, the N—H···O hydrogen bonds are red-shifted.

red-shifted H-bond, blue-shifted H-bond, AIM topological analysis, NBO analysis

The deepening investigation on the nature of hydrogen bond is of importance since hydrogen bond is present in many chemical, physical and biological systems[1−3]. For this purpose quantum chemistry calculation is an effective way[4]. Blue-shifted hydrogen bond has attracted much attention since it was confirmed by theory and experiments[5−10]. Many plausible mechanisms have been proposed in interpreting this unusual phenomenon[11−17]. Hobza et al.[11] proposed that there was difference in nature between blue-shifted and red-shifted hydrogen bonds. For the normal X—H···Y red-shifted hydrogen bonds, electron transfers from the lone pair electron of electron donator to the σ^*(X—H) of the electron acceptor, which elongates the X—H bond and leads to a red shift. For the blue-shifted hydrogen bonds, there are two steps in the process. First, owning to hyperconjugation, the electron is transferred to the other parts of the electron acceptor, which elongates the other bonds of the acceptor. Second, the electron acceptor undergoes a structural reorganization which contributes to the X—H contraction and blue shift of stretching frequency. Some other researchers considered that there was no difference between the blue-shifted and red-shifted hydrogen bonds in nature[13−17]. Alabugin et al.[16] have recently shown that structural reorganization of X—H bond in the process of both blue-shifted and red-shifted hydrogen bonds

Received June 3, 2005; accepted March 24, 2006
doi: 10.1007/s11426-007-2032-2
†Corresponding author (email: yongyang@aiofm.ac.cn)
Supported by the National Natural Science Foundation of China (Grant No. 20477043) and Knowledge Innovation Program by Chinese Academy of Sciences (KJCX2-SW-H08)

is determined by the balance of the opposing effects: X—H bond elongating effect due to hyperconjugative n(Y) → σ^*(X—H) interaction and X—H bond shortening effect due to rehybridization. When the elongating effect plays the dominant role, there is red shift; otherwise, blue shift.

It should be noted that both theoretical and experimental researches on blue-shifted hydrogen bonds were mainly concentrated on the C—H bond and very scarcely on the N—H bond. Alabugin et al.[16] predicted that the N—H···Y blue-shifted hydrogen bond was possible if hyperconjugation was quite weak (<13 kJ·mol^{-1}). Both Hobza and Li et al.[15,18] have predicted a blue-shifted N—H···F H-bond existing in complex NHF_2···HF at the MP2/6-31G(d,p) and MP2/6-311+G(d,p), respectively. However, the blue shifts observed in their work are quite small, only 13 and 17 cm^{-1}, respectively. In the present work, we have observed remarkable blue shifts (>100 cm^{-1}) of the N—H bond in the HCHO···HNO and HCOOH···HNO complexes where hyperconjugation is more than 21 kJ·mol^{-1}. It is in disagreement with the prediction proposed by Alabugin. In addition, the mechanism of N—H···O blue-shifted and red-shifted hydrogen bonds in different complexes is discussed.

1 Computational methods

The structures and vibrational frequencies of the complexes were investigated using both standard and counterpoise-corrected[19,20] (CP) optimization at the MP2/6-31+G(d,p), MP2/6-311++G(d,p), B3LYP/6-31+G(d,p) and B3LYP/6-311++G(d,p) levels, respectively. The basis set superposition errors (BSSE) were calculated according to the counterpoise method proposed by Boys and Bernardi[20]. The partial optimizations on the HNO monomer were performed at MP2/6-31+G(d,p) and MP2/6-311++G(d,p) levels. According to Onsager model, the SCRF calculations on the HNO monomers and complex B were carried out at B3LYP/ 6-31+G(d,p) level. Atoms in molecules (AIM)[21] analysis were also carried out at the MP2/6-31+G(d,p) level. Natural bond orbital (NBO)[22] analysis was performed at the MP2/6-31+G(d,p) level. All the calculations are performed using the Gaussian 03 program packages.

2 Results and discussion

2.1 Geometries, frequencies and energies

All optimized complexes are described in Figure 1. The characteristics of the complexes determined by both standard and CP optimization procedures at MP2/6-31+G(d,p), MP2/6-311++G(d,p), B3LYP/6-31+G(d,p) and B3LYP/6-311++G(d,p) levels are presented in Tables 1 and 2. As depicted in Figure 1, there is an N—H···O hydrogen bond and an X—H···Y (X=O and C; Y=F, N and O) hydrogen bond in all the complexes simultaneously, forming cyclic structures. For complexes A and B, the bond length (N2—H1) obtained by MP2 method agrees well with that obtained by B3LYP method. Similar results can also be found for the other complexes C, D, E and F. According to the basis sets effect, it can be seen that there is inconspicuous effect on the optimized structures. Owing to the existence of BSSE, the interaction energies are overestimated by the standard calculations[19]. In order to eliminate this effect, the CP-corrected calculations were performed. Compared to the standard calculations, the bond lengths obtained by CP-corrected calculations are obviously longer.

As shown in Table 2, the bond lengths (N1—H2 or N1—H3) in complexes C, D, E and F are longer than those in the monomers and corresponding stretching frequencies are lower, indicating the red-shifted N—H···O hydrogen bonds. On the contrary, the bond lengths (N1—H2) in complexes A and B contract relative to those in the monomers and corresponding stretching frequencies increase, which indicate that there are blue shifts. All calculations show the blue shifts are up to 144 cm^{-1} at most and up to 108 cm^{-1} at least. Although it has been predicted that a blue-shifted N—H···F H-bond exists in the NHF_2···HF complex, the corresponding blue shift is only 13 cm^{-1} at MP2/6-311+G(d,p) level[15].

The intermolecular interaction energies with both BSSE correction and ZPE correction are listed in Table 2. As shown in Table 2, the BSSE corrected and ZPE corrected energies are relatively large. The results indicate that BSSE correction and ZPE correction are important to accurately describe the intermolecular interaction energies. Among all complexes, complex D is the most stable and complex C is the most unstable.

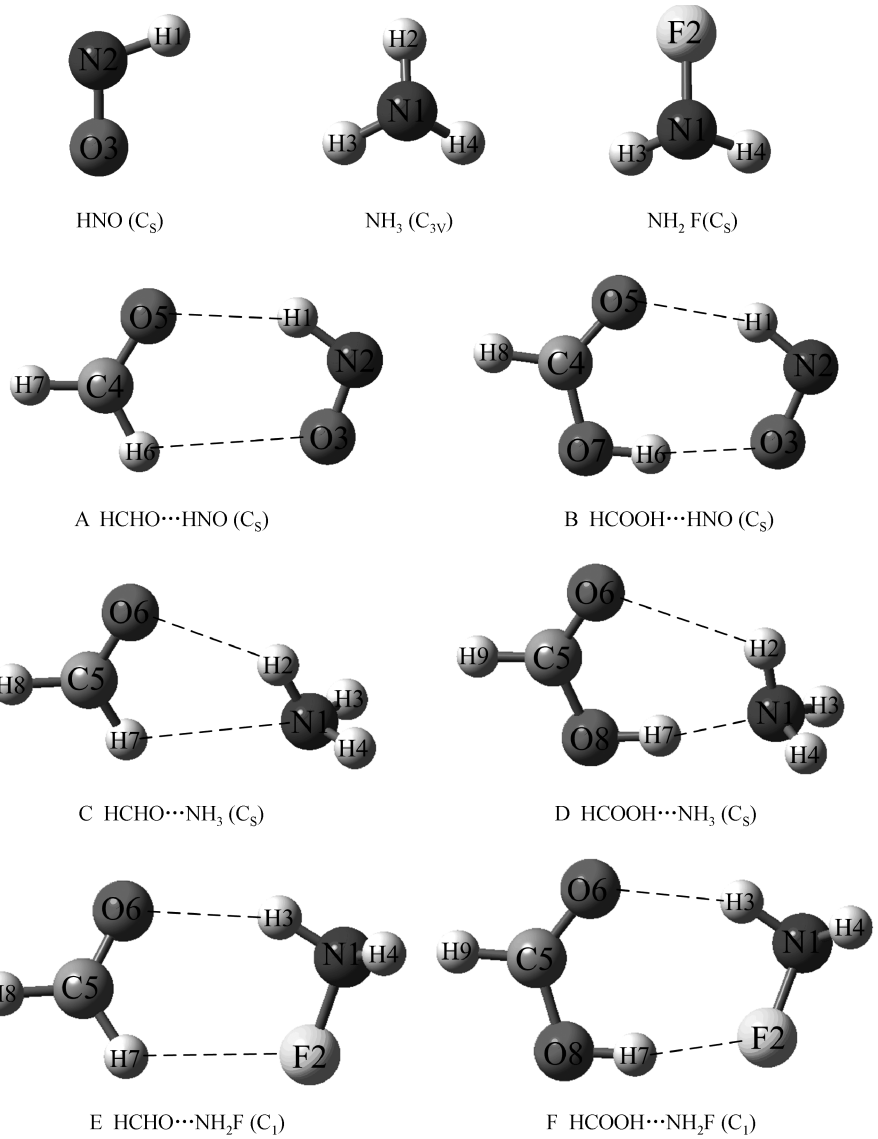

Figure 1 The optimized structure of the monomers and complexes.

2.2 AIM analysis

In order to shed light on the nature of the hydrogen bonds, the electron density topological analysis of the six complexes was performed at MP2/6-31+G(d,p) level. According to the AIM theory proposed by Bader[21], the topological characteristics of electron density depend on the grads vector of electron density ($\nabla\rho(r)$) and Laplacian of electron density ($\nabla^2\rho(r)$) values. Here, $\nabla^2\rho = \lambda_1 + \lambda_2 + \lambda_3$, λ_i's is an eigenvalue of the Hessian matrix of ρ. Then, when one of the three λ_i's is positive and the other two are negative, we denote it by (3, –1) and call it the bond critical point (BCP). When one of the three λ_i's is negative and the other two are positive, we denote it by (3,+1) and call it the ring critical point (RCP), which indicates the existence of a ring structure. ρ is used to describe the strength of a bond and $\nabla^2\rho$ describes the characteristic of the bond. Usually, the larger the value of ρ is, the stronger the bond is. Popelier et al.[23,24] proposed eight criteria for judging the existence of hydrogen bonds, among which three were the most fundamental and often applied, as Lipkowski et al.[25] pointed out. These three fundamental criteria are: the existence of a bond critical point, the electron density (ρ) and its Laplacian ($\nabla^2\rho$) values being in the range of 0.002—0.034 and 0.02—0.14 a.u., respectively.

The topological parameters of the bond critical point

Table 1 The partial parameters of optimized monomers and complexes (bond length: Å)

		MP2/6-31+G(d,p)		MP2/6-311++G(d,p)		B3LYP/6-31+G(d,p)		B3LYP/6-311++G(d,p)	
		Standard	CP	Standard	CP	Standard	CP	Standard	CP
HNO	*r*(N2－H1)	1.0508		1.0548		1.0638		1.0646	
	r(N2－O3)	1.2374		1.2212		1.2086		1.1997	
NH_3	*r*(N1－H2)	1.0114		1.0134		1.0157		1.0143	
NH_2F	*r*(N1－H3)	1.0195		1.0201		1.0238		1.0219	
	r(N1－F2)	1.4434		1.4193		1.4401		1.4336	
A	*r*(N2－H1)	1.0452	1.0453	1.0482	1.0486	1.0572	1.0575	1.0565	1.0570
	r(N2－O3)	1.2419	1.2415	1.2256	1.2252	1.2141	1.2141	1.2052	1.2052
	r(O5－H1)	2.2014	2.2707	2.2464	2.3117	2.1959	2.2233	2.2325	2.2336
	r(O3－H6)	2.7223	2.8168	2.7605	2.8645	2.7794	2.7946	2.7622	2.8115
B	*r*(N2－H1)	1.0457	1.0452	1.0483	1.0485	1.0577	1.0570	1.0569	1.0575
	r(N2－O3)	1.2428	1.2423	1.2270	1.2258	1.2173	1.2171	1.2088	1.2084
	r(O5－H1)	2.1024	2.1649	2.1362	2.2028	2.0445	2.0663	2.0637	2.0874
	r(O3－H6)	1.9183	1.9983	1.9196	2.0230	1.8694	1.8915	1.8859	1.9177
C	*r*(N1－H2)	1.0150	1.0142	1.0162	1.0157	1.0188	1.0186	1.0173	1.0171
	r(O6－H2)	2.3117	2.3727	2.3214	2.4072	2.3149	2.3349	2.3319	2.3446
	r(N1－H7)	2.5944	2.7366	2.6501	2.7350	2.6480	2.6809	2.6759	2.6975
D	*r*(N1－H2)	1.0163	1.0151	1.0173	1.0163	1.0196	1.0193	1.0183	1.0179
	r(O6－H2)	2.5447	2.5791	2.5794	2.6053	2.5581	2.5078	2.5517	2.5150
	r(N1－H7)	1.7427	1.8181	1.7507	1.8253	1.7116	1.7375	1.7503	1.7717
E	*r*(N1－H3)	1.0225	1.0219	1.0225	1.0220	1.0274	1.0273	1.0256	1.0253
	r(N1－F2)	1.4514	1.4509	1.4269	1.4259	1.4505	1.4501	1.4441	1.4436
	r(O6－H3)	2.1148	2.1896	2.1316	2.2171	2.0964	2.1223	2.1072	2.1301
	r(F2－H7)	2.5825	2.6855	2.6017	2.7200	2.6309	2.6467	2.5959	2.6412
F	*r*(N1－H3)	1.0236	1.0230	1.0237	1.0228	1.0298	1.0295	1.0279	1.0273
	r(N1－F2)	1.4599	1.4583	1.4353	1.4327	1.4622	1.4619	1.4554	1.4550
	r(O6－H3)	2.0907	2.1434	2.1146	2.1829	2.0379	2.0645	2.0514	2.0778
	r(F2－H7)	1.8707	1.9381	1.8801	1.9983	1.8376	1.8599	1.8630	1.8971

and ring critical point at the MP2/6-31+G(d,p) level are listed in Table 3. The values of ρ and $\nabla^2\rho$ for O5···H1 and O3···H6 in complexes A and B, O6···H2 and N1···H7 in complexes C and D, O6···H3 and F2···H7 in complexes E and F do fall within the proposed typical range of the hydrogen bonds. On the basis of the AIM topological analysis, we can claim that N—H···O and X—H···Y(X═O and C; Y═F, N and O) can be classified as hydrogen bonds. The strength of N—H···O in complexes B, E and F is relatively strong, while those of N—H···O in complexes C and D are relatively weak. These results are in good agreement with the O···H bond distances. In addition, there are RCPs in all the six complexes under investigation. A six-membered cyclic structure is observed for complexes A, D and E, a seven-membered cyclic structure can be seen in complexes B and F, and a five-membered cyclic structure appears for complex C.

2.3 NBO analysis

In order to investigate the mechanism on the blue-shifted or red-shifted hydrogen bonds, the NBO analysis was performed at MP2/6-31+G(d,p) level and the corresponding results are listed in Table 4. In the NBO analysis, the importance of hyperconjugative interaction and electron density transfer (EDT) from lone electron pairs of the Y atom to the X—H antibonding orbital in the X—H···Y system is well known, which leads to an increase in population of X—H antibonding orbital. The increase of electron density in X—H antibonding orbital

Table 2 The changes of bond lengths and bond stretching frequencies and the interaction energies for the complexes

		MP2/6-31+G(d,p)		MP2/6-311++G(d,p)		B3LYP/6-31+G(d,p)		B3LYP/6-311++G(d,p)	
		Standard	CP	Standard	CP	Standard	CP	Standard	CP
A	Δr(N2—H1) (Å)	–0.0056	–0.0055	–0.0066	–0.0062	–0.0066	–0.0063	–0.0081	–0.0076
	$\Delta \nu$(N2—H1) (cm^{-1})	+112	+108	+119	+113	+117	+112	+132	+127
	Δr(N2—O3) (Å)	+0.0045	+0.0041	+0.0044	+0.0040	+0.0055	+0.0055	+0.0055	+0.0055
	ΔE (kJ • mol^{-1})	–20.38	–20.17	–17.70	–17.49	–16.15	–16.15	–15.44	–15.44
	ΔE^{CP} (kJ • mol^{-1})	–15.44	–15.65	–13.47	–13.68	–14.73	–14.77	–13.72	–14.27
	$\Delta E^{CP,ZPE}$ (kJ • mol^{-1})	–9.46	–9.83	–8.12	–8.16	–8.74	–8.95	–7.78	–8.49
B	Δr(N2—H1) (Å)	–0.0051	–0.0056	–0.0065	–0.0063	–0.0061	–0.0068	–0.0077	–0.0071
	$\Delta \nu$(N2—H1) (cm^{-1})	+115	+120	+131	+127	+125	+132	+144	+136
	Δr(N2—O3) (Å)	+0.0054	+0.0049	+0.0058	+0.0046	+0.0087	+0.0085	+0.0091	+0.0087
	ΔE (kJ • mol^{-1})	–36.94	–36.57	–33.01	–32.51	–35.23	–35.19	–33.76	–33.72
	ΔE^{CP} (kJ • mol^{-1})	–28.70	–29.08	–25.65	–26.15	–32.64	–32.51	–31.00	–31.46
	$\Delta E^{CP,ZPE}$ (kJ • mol^{-1})	–19.12	–19.96	–16.99	–17.49	–22.84	–22.97	–21.42	–22.05
C	Δr(N1—H2) (Å)	+0.0036	+0.0028	+0.0028	+0.0023	+0.0031	+0.0029	+0.0030	+0.0028
	$\Delta \nu$(N1—H2) (cm^{-1})	–26, –38	–19, –28	–20, –30	–14, –23	–21, –30	–18, –27	–19, –28	–18, –26
	ΔE (kJ • mol^{-1})	–17.66	–17.24	–16.28	–16.07	–13.85	–13.81	–12.80	–12.76
	ΔE^{CP} (kJ • mol^{-1})	–13.26	–13.56	–12.18	–12.38	–12.59	–12.80	–11.80	–12.01
	$\Delta E^{CP,ZPE}$ (kJ • mol^{-1})	–6.49	–7.24	–5.69	–6.40	–5.82	–6.23	–5.40	–5.61
D	Δr(N1—H2) (Å)	+0.0049	+0.0037	+0.0039	+0.0029	+0.0039	+0.0036	+0.0040	+0.0036
	$\Delta \nu$(N1—H2) (cm^{-1})	–31, -46	–21, –33	–24, –38	–15, –26	–18, –30	–17, –27	–21. –33	–20, –28
	ΔE (kJ • mol^{-1})	–54.52	–53.97	–51.25	–50.75	–53.18	–53.05	–49.75	–49.62
	ΔE^{CP} (kJ • mol^{-1})	–43.01	–43.56	–41.17	–41.67	–48.4`	–48.37	–45.65	–46.11
	$\Delta E^{CP,ZPE}$ (kJ • mol^{-1})	–43.10	–35.02	–32.59	–33.18	–39.46	–39.83	–37.03	–37.61
E	Δr(N1—H3) (Å)	+0.0030	+0.0024	+0.0024	+0.0019	+0.0036	+0.0035	+0.0037	+0.0034
	$\Delta \nu$(N1—H3) (cm^{-1})	–23, –19	–13, –13	–17, –15	–10, –9	–29, –19	–27, –18	–30, –20	–27, –18
	Δr(N1—F2) (Å)	+0.0080	+0.0075	+0.0076	+0.0066	+0.0104	+0.0100	+0.0105	+0.0100
	ΔE (kJ • mol^{-1})	–23.51	–23.64	–21.51	–21.05	–19.58	–19.54	–19.37	–19.33
	ΔE^{CP} (kJ • mol^{-1})	–18.16	–18.58	–16.07	–16.57	–18.20	–18.33	–18.03	–17.87
	$\Delta E^{CP,ZPE}$ (kJ • mol^{-1})	–12.64	–13.35	–10.08	–11.55	–12.68	–12.84	–12.55	–12.43
F	Δr(N1—H3) (Å)	+0.0041	+0.0035	+0.0036	+0.0027	+0.0060	+0.0057	+0.0060	+0.0054
	$\Delta \nu$(N1—H3) (cm^{-1})	–28, –19	–19, –13	–23, –16	–14, –10	–53, –21	–49, –21	–50, –21	–45, –19
	Δr(N1—F2) (Å)	+0.0162	+0.0145	+0.0160	+0.0134	+0.0221	+0.0218	+0.0218	+0.0214
	ΔE (kJ • mol^{-1})	–37.07	–36.65	–34.43	–33.72	–34.81	–34.73	–34.50	–34.43
	ΔE^{CP} (kJ • mol^{-1})	–29.71	–30.12	–26.36	–27.15	–32.89	–32.64	–31.51	–31.92
	$\Delta E^{CP,ZPE}$ (kJ • mol^{-1})	–23.10	–23.68	–19.96	–21.09	–26.32	–36.15	–25.10	–25.61

weakens the X—H bond, which leads to its elongation and concomitant red shift of X—H stretching frequency. In general, the larger the hyperconjugative n(Y) → σ^*(X—H) interaction, the larger the electron density increase in the σ^*(X—H), and the X—H bond length elongation becomes more obvious. From Table 4, the hyperconjugative n(O5) → σ^*(N2—H1) interaction in complex A is larger than the hyperconjugative n(O6) → σ^*(N1—H2) interaction in complex C, however, the σ^*(N1—H2) electron density increase in complex A is obviously smaller than that in the σ^*(N1—H2) in complex C. Comparing the monomers HNO, NH_2F and NH_3, we can see that for monomer HNO the hyperconjugative n_2(O3)→σ^*(N2—H1) interaction is up to 61.21 kJ·mol^{-1} and the electron density in the σ^*(N2—H1) is up to 0.02462e. For the monomer NH_2F, the hyperconjugative n(F2)→ σ^*(N1—H3) interaction is relatively small and σ^*(N1—H3) electron density is 0.00492e. However, for NH_3, the electron density of σ^*(N1—H2) is 0.0e. It should be remarked that the hyperconjugative n(O3)→σ^*(N2—H1) interactions in complexes A and B are obviously lower than those in the HNO monomers from Table 4, which indicates a strong electron density redistribution in the electron acceptor HNO. Owing to

Table 3 Topological parameters of the bond critical point and ring critical point at the MP2/6-31+G(d,p) level

	BCP	ρ	$\nabla^2\rho$	λ_1	λ_2	λ_3
A	O5—H1	0.01565	0.04824	–0.01898	–0.01804	0.08526
	O3—H6	0.00607	0.02509	–0.00572	–0.00510	0.03591
B	O5—H1	0.01905	0.05680	–0.02357	–0.02254	0.10290
	O3—H6	0.02437	0.08036	–0.03406	–0.03231	0.14670
C	O6—H2	0.01243	0.04416	–0.01359	–0.01303	0.07077
	N1—H7	0.00947	0.03196	–0.00882	–0.00708	0.04786
D	O6—H2	0.00922	0.03651	–0.00867	–0.00488	0.05006
	N1—H7	0.03854	0.11607	–0.07269	–0.07264	0.26140
E	O6—H3	0.01812	0.05664	–0.02274	–0.02102	0.10100
	F2—H7	0.00624	0.03125	–0.00650	–0.00572	0.04347
F	O6—H3	0.01867	0.05895	–0.02291	–0.02204	0.10390
	F2—H7	0.02263	0.08659	–0.03280	–0.03111	0.15050
	RCP					
A	C4—O5—H1—N2—O3—H6	0.00503	0.02701	–0.00395	0.00450	0.02646
B	C4—O5—H1—N2—O3—H6—O7	0.00648	0.03236	–0.00536	0.00743	0.03028
C	C5—O6—H2—N1—H7	0.00748	0.04044	–0.00632	0.00893	0.03782
D	C5—O6—H2—N1—H7—O8	0.00859	0.03796	–0.00726	0.00775	0.03747
E	C5—O6—H3—N1—F2—H7	0.00435	0.02875	–0.00234	0.00656	0.02453
F	C5—O6—H3—N1—F2—H7—O8	0.00616	0.03052	–0.00487	0.00678	0.02861

the electron density redistribution, in complexes A and B, electrons are transferred from n(O5) to σ^*(N2—H1) firstly, then most electrons in the σ^*(N2—H1) are transferred to n(O3), which greatly weakens N2—H1 bond length elongation. For complexes C and D, the electron is completely transferred to the σ^*(N1—H2) because there are no electron density redistribution effects. For complexes E and F, the electron density redistribution is relatively weak, therefore, most electrons are transferred to σ^*(N1—H3) and a small part of electrons are transferred to the n(F2). From the above analysis, it can be concluded that the electron density redistribution primarily depends on the characteristics of the monomers. Generally, the larger electron density in σ^*(X—H) leads to the stronger electron density redistribution, as a consequence, the X—H bond length elongation is more effectively inhibited. This well explains why in complexes A and B, the σ^*(N2—H1) electron density increase is relatively small although the hyperconjugative n(O5) → σ^*(N2—H1) interaction is rather large.

Alabugin et al.[16] have recently proposed that rehybridization is the main factor for the H-bond blue shifts. In their opinion, the positive charge of the H atom in the X—H· · ·Y hydrogen bonds is more than that in the monomer; according to Bent's rule, rehybridization increases the s-character of X—H bond, strengthens its polarization, and consequently, shortens the X—H bond. Seen from Table 4, our results coincide well with the results of rehybridization. In all the complexes under investigation, the positive charges on the H atom of N2—H1 (N1—H2 and N1—H3) increase, so do the s-character of the hybrid orbital in N2—H1 (N1—H2 and N1—H3) and the polarizations. The s-character in N2—H1 of complexes A and B is more noticeably increased than those of the other complexes owing to the lower s-characters and stronger rehybridization in HNO monomer than in NH_3 and NH_2F monomers. This is in good agreement with the results through comparing CH_4 with C_2H_2 by Alabugin et al.[16].

2.4 Comparison to other theory

Hobza et al.[11] proposed that there was difference in nature between the red-shifted and blue-shifted hydrogen bonds and the structural reorganization is the fundamental reason for the blue-shifted H-bond. As listed in Table 2, the bond lengths (N2—O3) in HNO and bond lengths (N1—F2) in NH_2F are evidently elongated in complexes A, B, E and F. N2—H1···O5 hydrogen bonds in complexes A and B are blue-shifted, while N1—H3···O6 in complexes E and F are red-shifted, therefore, the structure reorganization should not be the natural difference between the red-shifted and blue-shifted hydrogen bonds. In order to deepen the understanding of the structural reorganization effect on the blue shift of N—H bond, the partial optimization on the HNO monomer was performed at MP2/6-31+G(d,p) and MP2/6-311++ G(d,p) levels. In this process, we optimized the

Table 4 NBO analysis of the monomers and complexes at the MP2/6-31+G(d,p) level

	HNO	A	B
n_1(O5) →σ^* (N2—H1) (kJ • mol^{-1})	–	10.38	17.45
n_2(O5) →σ^* (N2—H1) (kJ • mol^{-1})	–	15.06	20.59
n_1(O3) →σ^* (N2—H1) (kJ • mol^{-1})	–	–	14.64
n_2(O3) →σ^* (N2—H1) (kJ • mol^{-1})	61.21	49.87	27.28
σ^* (N2—H1) (e)	0.02462	0.02697	0.02979
$\Delta\sigma^*$ (N2—H1) (e)	–	0.00235	0.00517
q(H1) (e)	0.32756	0.36120	0.37174
Δq(H1) (e)	–	0.03364	0.04418
spn(N2—H1)	sp3.52	sp3.11	sp3.00
% s-char	22.10%	24.27%	24.96%
pol N2%	67.23%	69.04%	69.68%
(σ_{N2-H1}), H1%	32.77%	30.96%	30.32%
	NH_3	C	D
n_1(O6) →σ^* (N1—H2) (kJ • mol^{-1})	–	2.85	1.55
n_2(O6) →σ^* (N1—H2) (kJ • mol^{-1})	–	10.08	3.56
σ^* (N1—H2) (e)	0.00000	0.00455	0.00214
$\Delta\sigma^*$ (N1—H2) (e)	–	0.00455	0.00214
q(H2) (e)	0.39101	0.41193	0.43218
Δq(H2) (e)	–	0.02092	0.04117
spn(N1—H2)	sp2.75	sp2.63	sp2.71
% s-char	26.62%	27.51%	26.90%
pol N1%	69.59%	70.83%	71.72%
(σ_{N1-H2}), H2%	30.41%	29.17%	28.28%
	NH_2F	E	F
n_1(O6) →σ^* (N1—H3) (kJ • mol^{-1})	–	11.42	9.79
n_2(O6) →σ^* (N1—H3) (kJ • mol^{-1})	–	22.97	41.55
n_2(F2) →σ^* (N1—H3) (kJ • mol^{-1})	3.97	2.18	6.61
n_3(F2) →σ^* (N1—H3) (kJ • mol^{-1})	7.78	6.36	–
σ^* (N1—H3) (e)	0.00492	0.01425	0.01544
$\Delta\sigma^*$ (N1—H3) (e)	–	0.00933	0.01052
q(H3) (e)	0.37749	0.40665	0.41380
Δq(H3) (e)	–	0.02916	0.03631
spn(N1—H3)	sp2.88	sp2.56	sp2.52
% s-char	25.70%	28.07%	28.34%
pol N1%	69.05%	70.89%	71.27%
(σ_{N1-H3}), H3%	30.95%	29.11%	28.73%

HNO monomer with an elongated N—O bond taken from the optimized complex A and B, and this bond was kept frozen during the optimization. The results in Table 5 show that N2—O3 bond elongation can only lead to a small contraction in bond length and a slight blue shift in stretching frequencies of N2—H1. For complexes A and B, at the MP2/6-31+G(d,p) level the blue shifts are up to 112 and 115 cm^{-1}, while they are only 15 and 16 cm^{-1} due to the structural reorganizations. Therefore, we can exclude the possibility of the structural reorganization being the fundamental reason for the blue-shifted hydrogen bond.

Alabugin et al.[16] proposed that the blue-shifted and red-shifted hydrogen bonds were determined by the balance of the opposing effects: X—H bond elongating effect due to hyperconjugative n(Y)→σ^*(X—H) interaction and X—H bond shortening effect due to rehybridization. When X—H bond elongating effect is dominant, the X—H bond elongates. When X—H bond shortening effect is dominant, the X—H bond shortens. Further-

Table 5 The change between the partial optimized HNO and all optimized HNO of the bond lengths (N2—H1) and stretching frequencies at MP2/6-31+G(d,p) and MP2/6-311++G(d,p) levels

		MP2/6-31+G(d,p)	MP2/6-311++G(d,p)
A	Δr(N2—H1) (Å)	–0.0011	–0.0014
	$\Delta \nu$(N2—H1) (cm^{-1})	+15	+19
B	Δr(N2—H1) (Å)	–0.0012	–0.0016
	$\Delta \nu$(N2—H1) (cm^{-1})	+16	+22

more, Alabugin et al. suggested that red shift and blue shift are determined by the threshold which corresponds to the hyperconjugative n(Y)→ σ^*(X—H) interaction in the order of 13—21 kJ·mol^{-1}[16]. The red-shifted hydrogen bond is observed when the X—H bond elongating hyperconjugative n(Y)→σ^*(X—H) interaction is relatively strong (>21 kJ·mol^{-1}). The blue-shifted H-bond is likely to be observed only when the X—H bond elongating hyperconjugative n(Y)→σ^*(X—H) interaction is relatively weak (<13 kJ·mol^{-1}). However, our calculation shows that there are obviously blue-shifted (>100 cm^{-1}) N2—H1···O5 hydrogen bonds in complexes A and B in spite of the strong hyperconjugative n(O5) → σ^*(N2—H1) interaction(>21 kJ·mol^{-1}). The model proposed by Alabugin could not provide a reasonable explanation on this result. Besides the strong hyperconjugation in complexes A and B, we also notice the prominent electron density redistribution for the electron acceptor HNO, which can restrain the N2—H1 elongation. On the other hand, the more the hyperconjugation is, the stronger the rehybridization effect is. As a result, the increase in the s-character of spn hybrid orbital for the N2—H1 bond leads to intense contraction of the N2—H1 bond in complexes A and B. Consequently, the origins of blue-shifted H-bonds can be more clearly interpreted by our model.

On the basis of the above analyses, there are four factors affecting the red-shifted or blue-shifted hydrogen bonds: hyperconjugation, electron density redistribution, rehybridization and structural reorganization. Hyperconjugation contributes to the bond elongating effect, and the other three effects contribute to the bond shortening effect. It is worth pointing out that electron density redistribution and rehybridization are related to the character of the monomers. In general, the larger the electron density in σ^*(X—H), the stronger the electron density redistribution. The lower the s-character of spn hybrid orbital for the X—H bond, the stronger the rehybridization. On the other hand, with the hyperconjugation increasing, the bond elongating effect increases, so do the electron density redistribution and rehybridization. All these four effects contribute to the N2—H1(N1—H3) bond length changes in complexes A, B, E and F. The hydrogen bonds N2—H1···O5 in the complexes A and B are blue-shifted, while N1—H3···O6 in complexes E and F are red-shifted. Therefore, we completely agree with those who conclude that there are no fundamental differences between the red-shifted or blue-shifted hydrogen bonds. Among all six complexes, the electron density in σ^*(N—H) for HNO is the largest and the s-character of spn hybrid orbital for the N—H bond is lowest, so the N—H bond shortening effect is dominant, which leads to a large blue shift of stretching frequency. On the contrary, in complexes C, D, E and F, the elongating effects dominate resulting in red-shifted H-bonds.

2.5 Solvent effect on the structures, frequencies and interaction energies

In order to investigate the solvent effect on the structures, frequencies and interaction energies of monomers and complexes, the SCRF calculations were performed on the monomers and complexes at B3LYP/6-31+G(d,p) level (the relatively dielectric constants are 2.23, 8.93, 24.55, 32.63, 36.64 and 78.39, respectively). The corresponding results are summarized in Table 6. It is clear from the change of bond lengths given in Table 6 that solvent effect leads to decrease of the N2-H1 bond length in the HNO monomer. This behavior is more evident as ε is below 10.0. For complex B, the solvent effect on the structure is not significant. With the increase of ε, the O5—H1 bond length shows a slight contraction while the O3—H6 bond length has a small elongation. The N2—H1 bond length is almost independent of ε. As shown in Table 6, the solvent effects have a different influence on the geometries of complex B and the monomer HNO. As a result, the blue shift of the N2—H1 stretching frequency decreases as ε increases. At the B3LYP/6-31+G(d,p) level, the N2—H1

Table 6 The partial optimized parameters of HNO monomer and complex B in different solvents at B3LYP/6-31+G(d,p) levels

		ε = 2.23	ε = 8.93	ε = 24.55	ε = 32.63	ε = 36.64	ε = 78.39
HNO	r(N2—H1)(Å)	1.0624	1.0615	1.0614	1.0614	1.0614	1.0613
B	r(N2—H1)(Å)	1.0578	1.0579	1.0579	1.0579	1.0579	1.0579
	r(O5—H1)(Å)	2.0292	2.0112	2.0062	2.0055	2.0052	2.0041
	r(O3—H6)(Å)	1.8832	1.9006	1.9057	1.9065	1.9068	1.9080
	Δr(N2—H1)(Å)	–0.0046	–0.0036	–0.0035	–0.0035	–0.0035	–0.0034
	Δv(N2—H1)(cm^{-1})	+103	+84	+82	+82	+82	+81
	ΔE(kJ·mol^{-1})	–32.72	–30.38	–29.75	–29.62	–29.58	–29.50

blue shift is up to 125 cm^{-1} in the gas phase and 81 cm^{-1} in the liquid (ε = 78.39). In addition, we notice that the interaction energy in complex B shows a slight decrease with ε increasing.

1 Jeffrey G A. An Introduction to Hydrogen Bonding. New York: Oxford University Press, 1997
2 Desiraju G R, Steiner T. The Weak Hydrogen Bond. Oxford: Oxford University Press, 1999
3 Scheiner S. Hydrogen Bonding. New York: Oxford University Press, 1997
4 Hobza P, Zahradnik R. Intermolecular interactions between medium-sized systems. Nonempirical and empirical calculations of interaction energies: Successes and failures. Chem Rev, 1988, 88: 871—897
5 Delanoye S N, Herrebout W A, van der Veken B J. Blue shifting hydrogen bonding in the complexes of chlorofluoro haloforms with acetone-d_6 and oxirane-d_4. J Am Chem Soc, 2002, 124: 11854—11855
6 Hobza P, Havlas Z. The fluoroform···ethylene oxide complex exhibits a C—H···O anti-hydrogen bond. Chem Phys Lett, 1999, 303: 447—452
7 Boldeskul I E, Tsymbal I F, Ryltsev E V, et al. Reversal of the usual V(C—H/D) spectral shift of haloforms in some hydrogen-bonded complexes. J Mol Struct, 1997, 436: 167—171
8 Reimann B, Buchhold K, Vaupel S, et al. Improper, blue-shifting hydrogen bond between fluorobenzene and fluoroform. J Phys Chem A, 2001, 105: 5560—5566
9 Wang X, Zhou G, Tian A M, et al. *Ab initio* investigation on blue shift and red shift of C—H stretching vibrational frequency in NH_3···CH_nX_{4-n} (n=1,3, X=F, Cl, Br, I) complexes. J Mol Struc-Theochem, 2005, 718: 1—6
10 Li J, Xie D Q, Yan G S. Theoretical study of the intermolecular hydrogen bond interaction for furan-HCl and furan-$CHCl_3$ complexes. Sci China Ser B-Chem, 2003, 46(2): 113—118
11 Hobza P, Havlas Z. Blue-shifting hydrogen bonds. Chem Rev, 2000, 100: 4253—4264
12 van der Veken B J, Herrebout W A, Szostak R, et al. The nature of improper, blue-shifting hydrogen bonding verified experimentally. J Am Chem Soc, 2001, 123: 12290—12293
13 Gu Y, Kar T, Scheiner S. Fundamental properties of the CH···O interaction: Is it a true hydrogen bond? J Am Chem Soc, 1999, 121: 9411—9422
14 Hermansson K. Blue-shifting hydrogen bonds. J Phys Chem A, 2002, 106: 4695—4702
15 Li X, Liu L, Schlegel H B. On the physical origin of blue-shifted hydrogen bonds. J Am Chem Soc, 2002, 124: 9639—9647
16 Alabugin I V, Manoharan M, Peabody S, et al. Electronic basis of improper hydrogen bonding: A subtle balance of hyperconjugation and rehybridization. J Am Chem Soc, 2003, 125: 5973—5987
17 Yang Y, Zhang W J, Pei S X, et al. Blue-shifted and red-shifted hydrogen bonds: Theoretical study of the CH_3CHO···NH_3 complexes. J Mol Struc-Theochem, 2005, 732: 33—37
18 Hobza P. N—H···F improper blue-shifting H-bond. Int J Quantum Chem, 2002, 90: 1071—1074
19 Simon S, Duran M, Dannenbery J J. How does basis set superposition error change the potential surfaces for hydrogen-bonded dimers? J Chem Phys, 1996, 105: 11024—11031
20 Boys S F, Bernardi F. Calculations of small molecular interactions by differences of separate total energies. Some procedures with reduced errors. Mol Phys, 1970, 19: 553—556
21 Bader R W F. A quantum theory of molecular structure and its applications. Chem Rev, 1991, 91: 893—928
22 Reed A E, Curtiss L A, Weinhold F. Intermolecular interactions from a natural bond orbital, donor-acceptor viewpoint. Chem Rev, 1988, 88: 899—926
23 Koch U, Popelier P L A. Characterization of C—H—O hydrogen bonds on the basis of the charge density. J Phys Chem-US, 1995, 99: 9747—9754
24 Popelier P L A. Characterization of a dihydrogen bond on the basis of the electron density. J Phys Chem A, 1998, 102: 1873—1878
25 Lipkowski P, Grabowski S J, Robinson T L, et al. Properties of the C—H···H dihydrogen bond: An *ab initio* and topological analysis. J Phys Chem A, 2004, 108: 10865—10872